Source signature and static shifts estimations for multi-component ocean bottom data

Mandy Wong and Shuki Ronen

ABSTRACT

We present an interpretive study to estimate the source signature and source statics of a field ocean bottom dataset. We use the down-going direct arrival to extract the source signature at different offsets. The down-going wavefield is obtained from a simple summation of the pressure (P) and the vertical partical velocity (Z) of the multi-component data. Such a summation is scaled by a factor that depends on offset and is estimated directly from the amplitude of the P and Z values in the $t-x$ domain. In addition, we compare two approaches to estimating the source-side static shifts. Our static shifts estimation give satisfactory result for an absolute offset up to $\pm$5000 meters.

INTRODUCTION

Many migration algorithms, such as shot-profile, plane wave, and reverse time migration, require the input of source wavelets as part of the calculation. Ocean bottom data have a distinct advantage in the estimation of the source wavelet, because an ocean bottom seismometer and hydrophone can pick up the source signature as direct arrivals through a relatively homogeneous medium. As shown in figure 1, the source wave path only needs to go through the water once to reach the receivers.

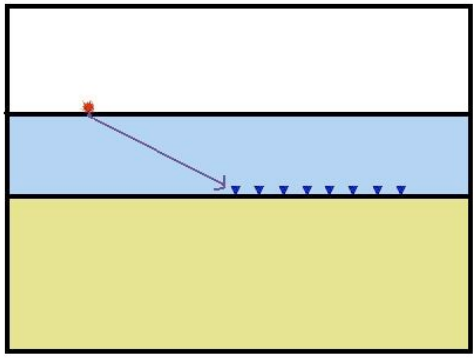

Figure 1: For ocean bottom data acquisition, the source wavelet is picked up by the down-going direct arrival data.[**NR**]

Source signatures are offset-dependent because each shot is generated from an array of airguns and the obliquity of the source wave path directly affects the shape of the

wavelet. A crude way to extract the source signature from a direct arrival is to time-window the pressure signal at the receiver. However, this technique is often inaccurate because the source bubble often overlaps with the recorded primary reflection. A better way to extract the source signature is to first separate the total data into up-going and down-going wavefields, and then perform time windowing only on the down-going component. We can do that because the direct arrival is strictly down-going, as illustrated in figure 1. For multi-component ocean bottom data, we can perform up-down separation using the pressure (P) and vertical velocity (Z) wavefields. This method is called PZ summation.

There is significant literature on the method of PZ summation to decompose data into up-going and down-going wavefields (Amundsen, 1993; Sonneland et al., 1986). Some methods involve separation in the $\tau - p$ or $\omega - k$ (Fourier) domain. However, transformation into other domains poses a problem when the data are aliased or sparsely sampled. In this study, we perform PZ summation in the physical (t-x) space to avoid this difficulty.

In the next section, we first present the field dataset and discuss some of the challenges. Futhermore, we estimate the source statics in a common receiver gather. Variations in shot deployment depth and the water column cause time anomalies that can be approximated as surface-consistent static time shifts. We compare two methods of static time shift estimation. One method uses the maximum pulse of the source while the other use cross-correlation. Finally, we discuss and show the result of the source signature extraction on the field dataset.

OCEAN BOTTOM NODES DATASET

The P (pressure) and Z (vertical velocity) components of an ocean bottom common receiver gather are shown in Figures 2. Data are acquired using ocean bottom nodes. The typical water depth in the surveyed area is around 500m with a soft sediment layer of 150m. From the raw data, we can identify direct arrivals, refraction, and water reverberations. There is an outcrop at the sea bottom to the left of the ocean bottom node (OBN) receiver. The dataset is spatially aliased, with 50 meters spacing between shots.

To focus on the source signal, we apply hyperbolic moveout (HMO) at a velocity of 1480m/s and time-window the data near the direct arrival (Figure 3). Linear moveout performs time-shifting ($\Delta\tau$) on each trace. Time shifts are offset-dependent and are calculated as shown in equation 1:

$$\Delta\tau = \sqrt{\tau_o^2 + \frac{x^2}{v^2}} - \tau_o, \tag{1}$$

where x is the full offset, v is the water velocity, and τ_o is the zero-offset arrival time. From Figure 3, we can see that the direct arrival is not perfectly flat. This non-flatness

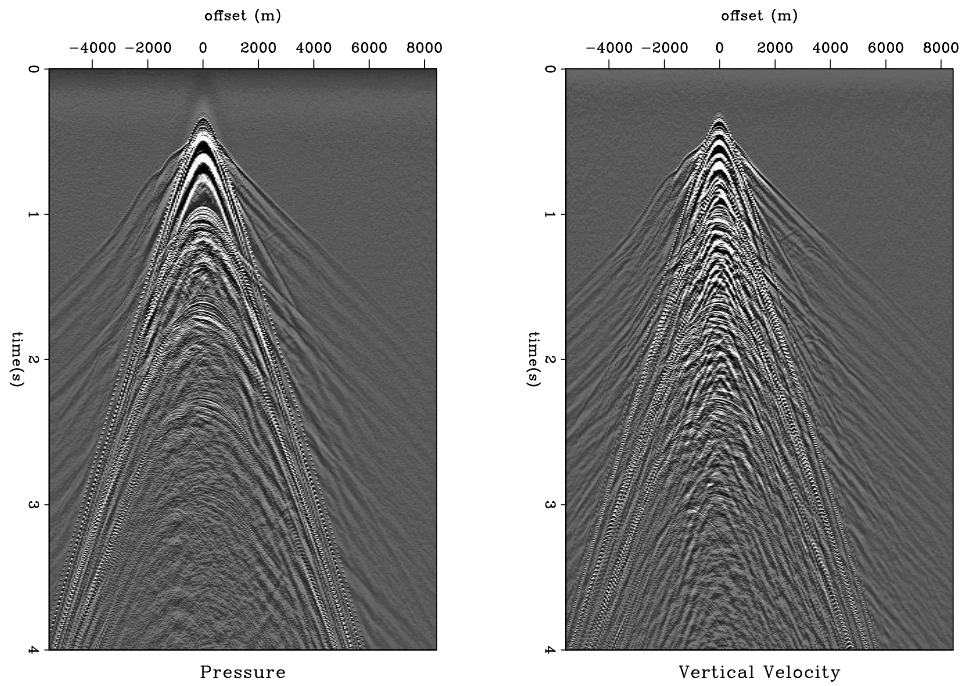

Figure 2: The left plot shows the pressure component and the right plot shows the vertical velocity component. From the raw data, we can identify direct arrivals, refraction, and water reverberations.[**ER**]

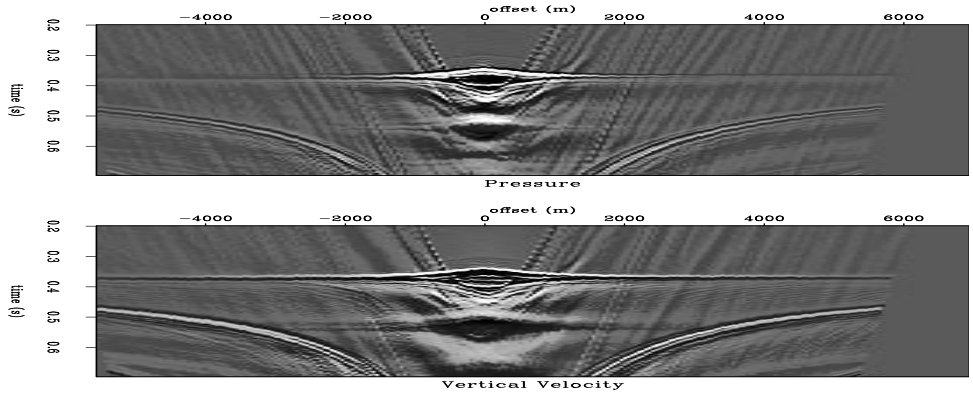

Figure 3: The top plot shows the pressure component and the bottom plot shows the vertical velocity component after hyperbolic moveout correction. The data are time-windowed around direct arrival.[**ER**]

indicates shot statics in this common-reciever gather. Shot statics can be caused by variations in deployment depth and cross-line displacement. Another noticeable feature is that primary reflections follow almost immediately after the direct arrivals. This causes difficulty, as primary signal would overlap with the source bubble signal. Next, we present two methods to estimate the source statics by flattening the HMO output.

STATIC SHIFTS CORRECTION

Correction using maximum pulse alignment

One way to calculate the static shifts correction is by aligning the maximum pulse of the source signature. A typical air-gun signature, including the effect of the source ghost, consists of a large pulse and its bubbles, as shown in Figure 4. Since the amplitude of the initial maximum pulse is much higher than the amplitude of the bubble, we can estimate the static correction by picking and aligning the time of the maximum pulse. The middle panel of figure 5 shows the z-component of the resulting direct-arrival after static shifts correction using this method.

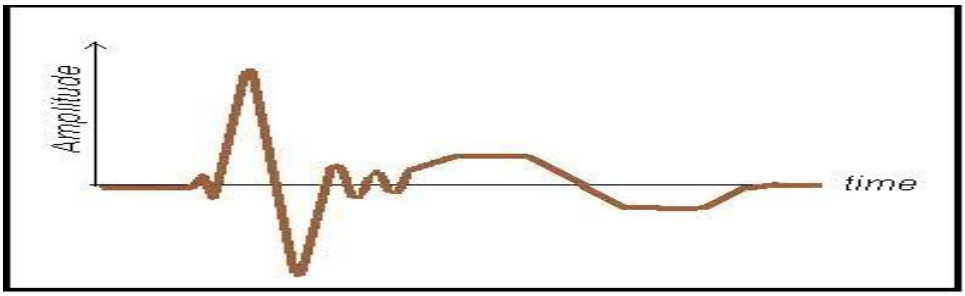

Figure 4: A typical air-gun signature consists of a large pulse and its bubbles. The negative signal comes from the source ghost. [**NR**]

Searching for the maximum pulse can be tricky for traces at large offset, as the amplitude of the pulse attenuates with a longer travel distance. Satisfactory results can be obtained up to an absolute offset of $\pm 5000m$. We have restricted the search neighborhood to be near the LMO time in order to alleviate this problem. The top panel of figure 6 shows the static shift calculated at different offsets by aligning the maximum pulse.

Correction using cross-correlation

Another way to estimate static shifts is to observe the cross-correlation of traces at different offsets with the zero-offset trace. In this way, the lag time that gives maximum cross-correlation would define the static shifts. The bottom panel of Figure 5 shows the resulting direct arrival after static shifts corrrection using this method.

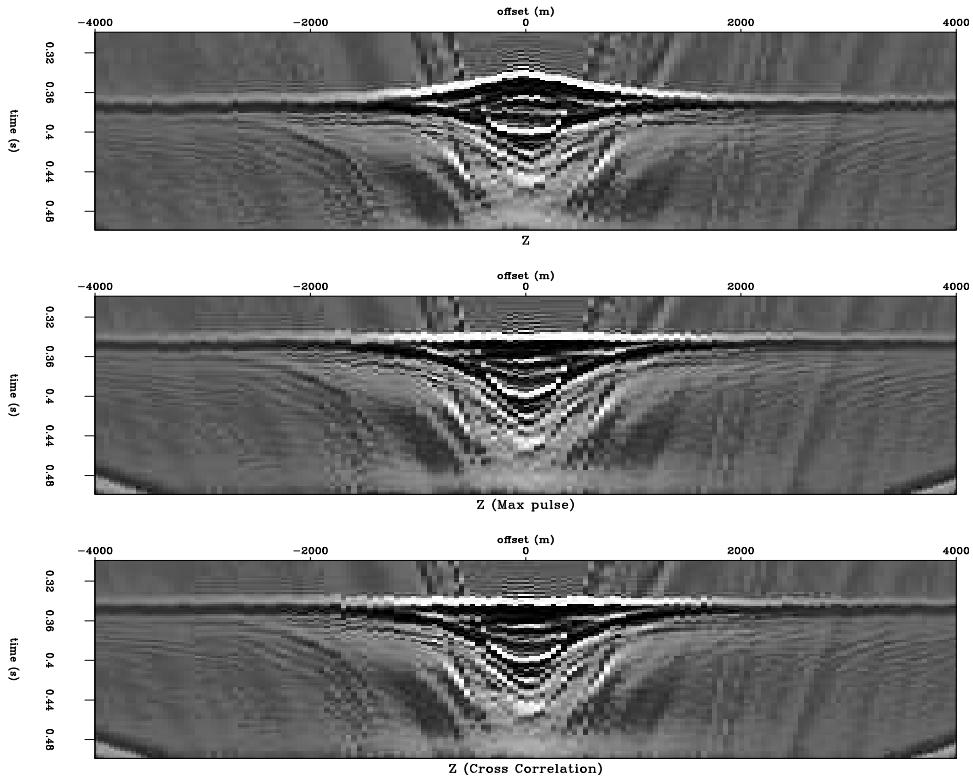

Figure 5: (Top) Vertical velocity before static shifts. (Middle) Vertical velocity after static shifts correction using maximum pulse alignment. (Bottom) Vertical velocity after static shifts correction using cross-correlation. [**ER**]

To maximize alignment around the direct arrival, we perform cross-correlation only in the neighborhood of the HMO time. Comparing the result from using the maximum pulse method and the cross-correlation method, we can see that the former method performs better. The bottom panel of Figure 6 shows the static shift calculated at different offsets by using the cross-correlation method. From the figure, we see that the direct arrival are better lined up in the region of ±1000 meters for the maximum pulse method.

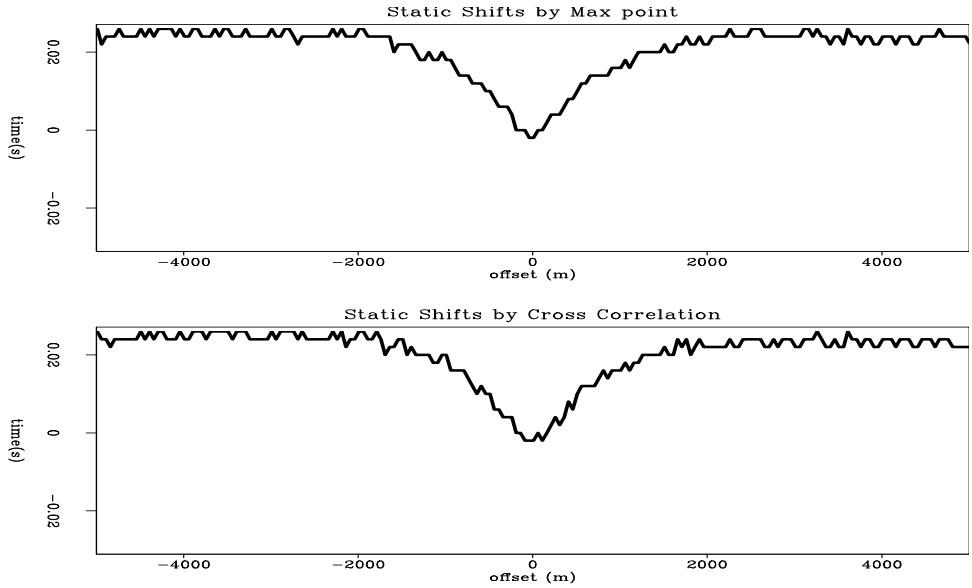

Figure 6: Static shifts estimated at different offsets (Top) using maximum pulse method and (bottom) cross-correlation method. [**ER**]

UP-DOWN SEPARATION USING PZ SUMMATION

Traditionally, PZ summation is employed to extract the up-going portion of the wavefield with the goal of eliminating water reverberation (Rosales and Guitton, 2004). We use the down-going wavefield to estimate the source wavelet at a different offset. For PZ summation, Barr and Sanders (1989) have derived a relation to model the up-going wavefield as shown in the following equation:

$$U(t,x) = \frac{1}{2}\left(P(t,x) + \frac{\rho v_p}{cos\gamma_p}\frac{k_t(1+k_r)}{(1-k_r)}Z(t,x)\right), \tag{2}$$

where $U(t,x)$ is the up-going wavefield, $P(t,x)$ is the pressure, $Z(t,x)$ is the vertical velocity, ρ is the water density, v_p is the P-wave water velocity, γ_p is the P-wave refraction angle at the sea bottom for upgoing wavefield, and k_r, k_t are the reflection coefficient and the refraction coefficient of the ocean bottom, respectively. One drawback of equation 2 is that it assumes that the reflection coefficent of the ocean

surface is -1, which is not always true. We have used a more data-driven approach in which a scaling factor between P and Z is fitted from the amplitude of their direct arrival, as described by equations 3 and 4.

From equation 2, we can see that the scaling factor in front of $Z(t,x)$ is offset-dependent. In this study, instead of calculating the scaling factor from equation 2, we fit for it from the amplitude of the pressure and vertical velocity components, time-windowed around the direct arrival:

$$\begin{aligned} U(t,x) &= \frac{1}{2}\left(P(t,x) + \text{scale}(x) z(t,x)\right), \\ D(t,x) &= \frac{1}{2}\left(P(t,x) - \text{scale}(x) z(t,x)\right), \end{aligned} \tag{3}$$

$$\text{scale}(x) = \frac{\sum_{t\in\Omega_t} \mid P(t,x) \mid}{\sum_{t\in\Omega_t} \mid Z(t,x) \mid}, \tag{4}$$

where scale(x) is the offset dependent scaling factor between pressure and vertical particle velocity, and Ω_t is the time-window near the direct arrival time. Figure 7 shows the scaling factor computed using equation 4. Figure 8 shows the resulting up-going and down-going signals after PZ summation. Notice that the up-going signal is much weaker than the down going signal.

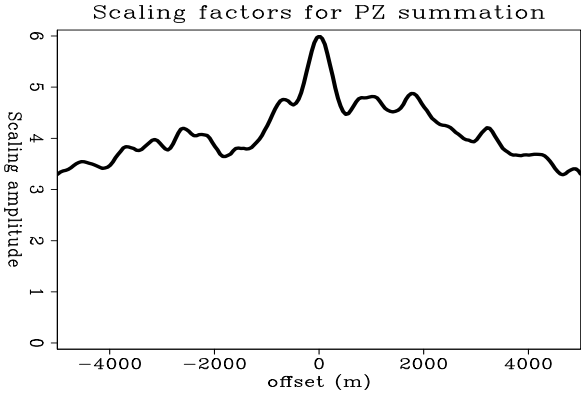

Figure 7: Scaling factor as a function of offset. It is estimated from the average amplitude of P over the average amplitude of Z [**ER**]

SOURCE SIGNATURE EXTRACTION

After obtaining the down-going wavefield, we can obtain an estimate of the source signature from the recorded amplitude of the direct arrival. Figure 9 shows several source wavelets at different offset values. For a near zero-offset wavelet, we can clearly identify the typical parts of a source wavelet, which include the source ghost and the

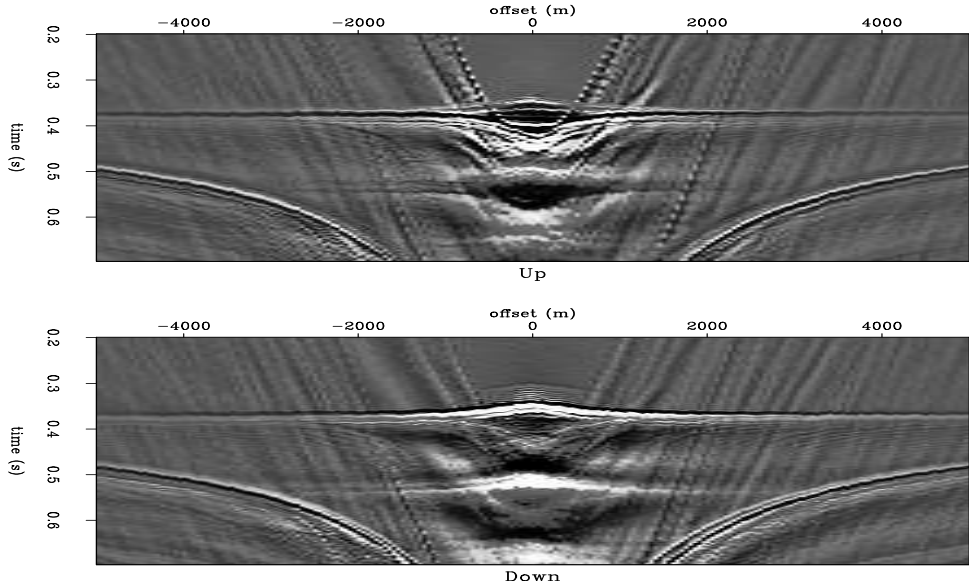

Figure 8: The top shows the resulting up-going wavefields and the bottom shows the down-going wavefields after PZ summation. [**ER**]

source bubble. The amplitude of the large negative pulse is less than that of the large positive pulse. This fact indicates that the reflection coefficient of the water surface is not exactly -1.

In Figure 9, we see that the amplitude and shape of the source wavelet change drastically with the offset. Primary reflections overpower some of the source signals. The source bubble can hardly be identified.

Next, we compare our result with another source wavelet that is independently estimated in the same survey. We can see the difference in the large negative pulse and the source bubbles.

CONCLUSIONS

We performed an interpretive study of a field ocean bottom dataset to extract its source signature as a function of the offset and to estimate the source statics. Source signatures are obtained by capturing the direct arrival signal for the down-going wavefields. PZ summation is performed in the t-x domain with a scaling factor that is fitted from the data. Source statics are estimated by correcting the deviations from the linear moveout time. We have used two methods of performing that correction. Shifts estimations are consistent between the two approaches at small offsets. Our approaches become limited at larger offsets. As the amplitude of the signature becomes weaker with offset, obtaining the source signature and estimating the static shifts become difficult.

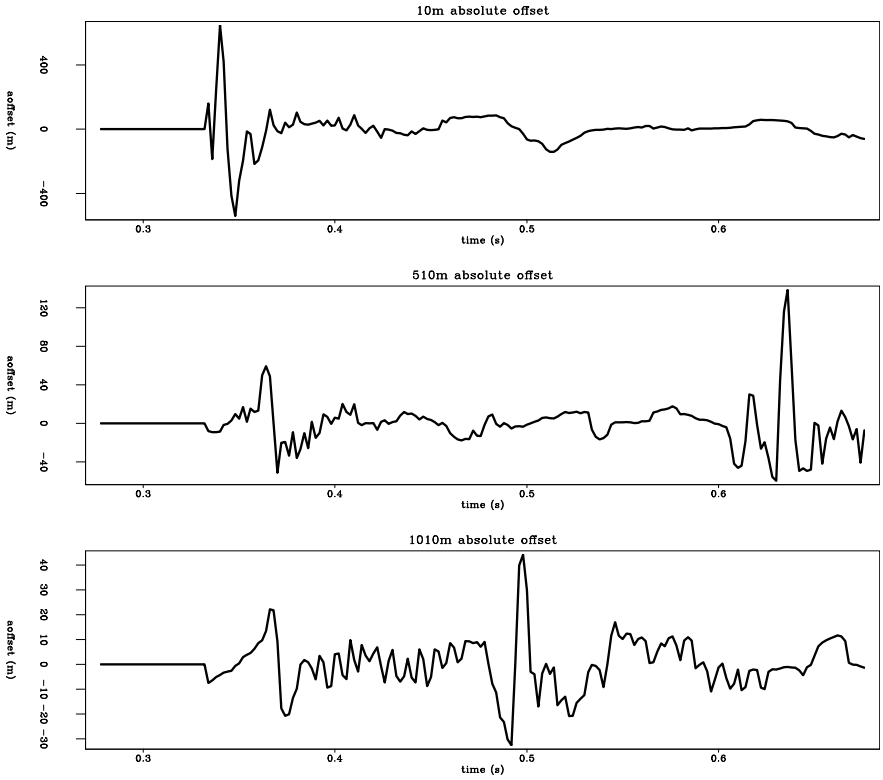

Figure 9: Source wavelets at different offset values. These wavelets are obtained from the amplitude of the down-going wavefields windowed near direct arrival time. [**ER**]

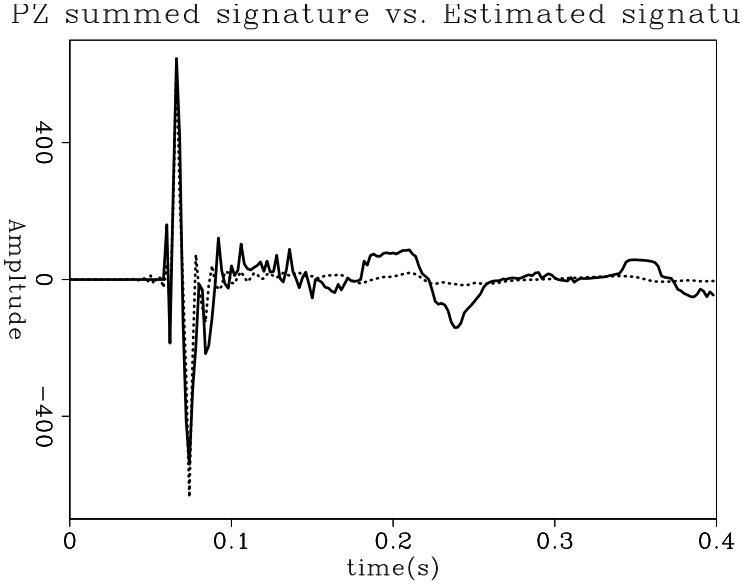

Figure 10: Comparison of our zero-offset source wavelet (solid line) with another wavelet independently estimated in the same survey (dashed line). Our wavelet indicates that the ocean surface reflection coefficent is not -1. Also, the amplitude of the source bubble is bigger. [**ER**]

ACKNOWLEDGMENTS

We thank SeaBird Explorations for the release of this field dataset. We also thank the sponsors of Stanford Exploration Project for funding this research.

REFERENCES

Amundsen, L., 1993, Wavenumber-based filtering of marine point-source data: Geophysics, **58**, 1335–1348.

Barr, F. J. and J. L. Sanders, 1989, Attenuation of water-column reverations using pressure and velocity detectors in a water-bottom cable: SEG Expanded Abstracts, **59**, 653–656.

Rosales, D. A. and A. Guitton, 2004, Ocean-bottom hydrophone and geophone coupling: SEP-Report, **115**, 57–70.

Sonneland, L., L. E. Berg, P. Eidsvig, A. Haugen, B. Fotland, and J. Vestby, 1986, 2-d deghosting using vertical receiver arrays: SEG Expanded Abstracts, **5**, 516.